● **RESEARCH ARTICLE**

Electroacupuncture alleviates cerebral ischemia and reperfusion injury *via* modulation of the ERK1/2 signaling pathway

Xiao-lu Jin[1, #], Peng-fei Li[2, #], Chun-bing Zhang[2, 3], Jin-ping Wu[3], Xi-lian Feng[1], Ying Zhang[1], Mei-hong Shen[1, *]

1 Second Clinical College, Nanjing University of Chinese Medicine, Nanjing, Jiangsu Province, China
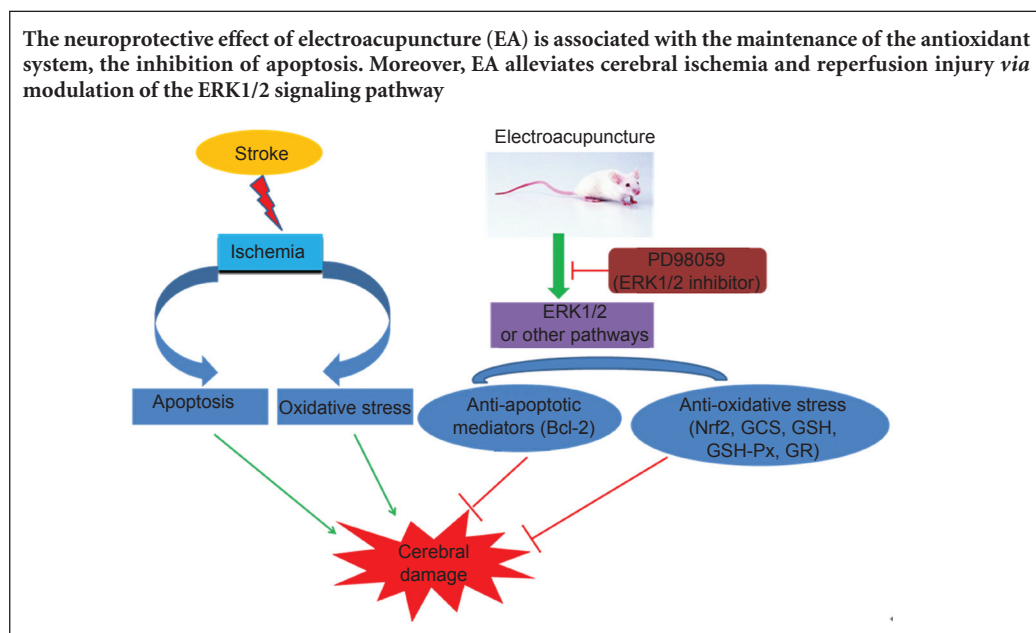2 Department of Clinical Laboratory, Jiangsu Province Hospital of Traditional Chinese Medicine, Affiliated Hospital of Nanjing University of Chinese Medicine, Nanjing, Jiangsu Province, China
3 College of Basic Medicine, Nanjing University of Chinese Medicine, Nanjing, Jiangsu Province, China

How to cite this article: Jin XL, Li PF, Zhang CB, Wu JP, Feng XL, Zhang Y, Shen MH (2016) Electroacupuncture alleviates cerebral ischemia and reperfusion injury via modulation of the ERK1/2 signaling pathway. Neural Regen Res 11(7):1090-1098.

Graphical Abstract

The neuroprotective effect of electroacupuncture (EA) is associated with the maintenance of the antioxidant system, the inhibition of apoptosis. Moreover, EA alleviates cerebral ischemia and reperfusion injury *via* modulation of the ERK1/2 signaling pathway

Correspondence to:
Mei-hong Shen, Ph.D.,
13815894855@163.com.

#*These authors contributed equally to this study.*

orcid:
0000-0002-8650-2778
(Mei-hong Shen)

Abstract

Electroacupuncture (EA) has anti-oxidative and anti-inflammatory actions, but whether the neuroprotective effect of EA against cerebral ischemia-reperfusion (I/R) injury involves modulation of the extracellular regulated kinase 1/2 (ERK1/2) signaling pathway is unclear. Middle cerebral artery occlusion (MCAO) was performed in Sprague-Dawley rats for 2 hours followed by reperfusion for 24 hours. A 30-minute period of EA stimulation was applied to both *Baihui* (DU20) and *Dazhui* (DU14) acupoints in each rat (10 mm EA penetration depth, continuous wave with a frequency of 3 Hz, and a current intensity of 1–3 mA) when reperfusion was initiated. EA significantly reduced infarct volume, alleviated neuronal injury, and improved neurological function in rats with MCAO. Furthermore, high mRNA expression of *Bax* and low mRNA expression of Bcl-2 induced by MCAO was prevented by EA. EA substantially restored total glutathione reductase (GR), glutathione (GSH) and glutathione peroxidase (GSH-Px) levels. Additionally, Nrf2 and glutamylcysteine synthetase (GCS) expression levels were markedly increased by EA. Interestingly, the neuroprotective effects of EA were attenuated when ERK1/2 activity was blocked by PD98059 (a specific MEK inhibitor). Collectively, our findings indicate that activation of the ERK1/2 signaling pathway contributes to the neuroprotective effects of EA. Our study provides a better understanding of the regulatory mechanisms underlying the therapeutic effectiveness of EA.

Key Words: nerve regeneration; electroacupuncture; ischemia and reperfusion injury; middle cerebral artery occlusion; mitogen-activated protein kinase; oxidative stress; nuclear factor erythroid 2-related factor 2; glutamylcysteine synthetase; glutathione reductase; B cell lymphoma 2; glutathione peroxidase

Introduction

Stroke, a common cerebrovascular disease, has high morbidity and mortality (Russo et al., 2011). The sudden blockade of a blood vessel by a thrombus or embolism results in ischemic stroke in more than 80% of patients (Donnan et al., 2008). Although the mechanisms underlying cerebral ischemia and reperfusion (I/R) injury are not fully clear, there is accumulating evidence that oxidative stress plays a major role in the pathogenic process (Allen and Bayraktutan, 2009). Excessive elevation of free radicals and reactive oxygen species (ROS) during cerebral I/R activates several signaling pathways and increases oxidative stress (Deb et al., 2010).

Acupuncture regulates body homeostasis and induces major physiological changes. It has been shown that electrical stimulation (electroacupuncture, EA) exhibits neuroprotective effects, and has been widely applied for the treatment of ischemic stroke in experimental animals and clinical practice (Wu et al., 2010; Wang et al., 2011). Although there are numerous mechanistic studies of EA focusing on neural pathways, regulation and neural responses (Tjen-A-Looi et al., 2006; Li et al., 2010), the mechanisms of neuroprotection remain unclear. A number of recent studies have shown that EA exerts anti-oxidative and anti-inflammatory effects that alleviate renal injury (Yu et al., 2015), lung injury (Yu et al., 2014) and Parkinson's disease (Lv et al., 2015). These effects of EA appear to be mediated *via* the activation of the nuclear factor erythroid 2-related factor 2 (*Nrf2*) pathway. Several reports have also demonstrated that EA activates the PI3K/Akt and ERK1/2 signaling pathways or suppresses intracellular ERK and p38MAPK signaling to help repair spinal cord injury (Renfu et al., 2014) and alleviate neuropathic pain (Wang et al., 2015). Previous studies from our research group have shown that EA protects against oxidative stress (Li et al., 2005). However, it is not known whether the neuroprotective action of EA in cerebral I/R injury is mediated through the modulation of the ERK1/2 pathway. The aim of this study was to investigate the neuroprotective effect of EA in the rat model of middle cerebral artery occlusion (MCAO) and determine whether the therapeutic effect of EA is associated with the regulation of the ERK1/2 pathway.

Materials and Methods

Ethics statement

The animal studies were approved by the Animal Care and Use Committee of the Institute of Nanjing University of Chinese Medicine, and were performed in accordance with the National Institutes of Health Guide for the Care and Use of Laboratory Animals. Efforts were made to minimize suffering and the number of animals used in each experiment.

Animals

A total of 50 specific-pathogen-free adult male Sprague-Dawley rats, weighing 280–320 g, were provided by SLRC Laboratory Animals (Shanghai, China) (certification No. SCXK (Hu) 2007-0005) and housed under diurnal lighting conditions (12-hour light/dark cycle) for at least 1 week be-fore surgery. Rats were randomly divided into the following five groups (*n* = 10 for each group): normal, sham-operation (sham), MCAO, MCAO + EA (EA), and MCAO + EA + PD98059 (EA plus PD98059) groups.

MCAO model establishment

Rats were allowed free access to food and water, but were fasted 12 hours before surgery. All animals were anesthetized by intraperitoneal injection of 10% chloral hydrate (Abbott, North Chicago, IL, USA). The MCAO model was performed as described previously, with minor modifications (Li and Cui, 2006). Briefly, the right common carotid artery, internal carotid artery and external carotid artery were exposed through a ventral midline neck incision. The internal carotid artery was then isolated and coagulated, and the proximal common carotid artery was ligated. A 4-0 monofilament nylon suture (Beijing Sunbio Biotech Co. Ltd., Beijing, China) with a rounded tip was inserted into the internal carotid artery from the common carotid artery through the external carotid artery stump and gently advanced 18 to 20 mm to occlude the middle cerebral artery. Core body temperature was maintained at 37.0 ± 0.5°C using a heating pad and heating lamp during the whole procedure. After 2 hours of MCAO, a neurological test was administered by an examiner blinded to the experimental groupings after MCAO using a modified scoring system based on that developed by Kuluz et al. (1993) as follows: 0, normal; 1, asymmetry of extension or abduction of the right upper extremity when lifted by the tail; 2, circling to the right during locomotion. A score of 2 was considered to indicate a successful model, and the suture was removed to restore blood flow (reperfusion). Rats in the sham group underwent identical surgery except that the suture was not inserted.

EA and PD98059 treatments

Stainless acupuncture needles, 0.3 mm in diameter (HuaTuo, Suzhou Medical Appliance Factory), were applied to both *Baihui* (DU20) (horizontal insertion of needle) and *Dazhui* (DU14) (oblique insertion of needle at an angle of 30°) acupoints in each rat (10 mm EA penetration depth, continuous wave with a frequency of 3 Hz, and a current intensity of 1–3 mA) (**Figure 1**), while the animals were undergoing reperfusion. The rats were acupunctured with an electrical needle stimulator (WQ1002K, Electro-Acupuncture Equipment Company, China) for 30 minutes.

Rats in the EA plus PD98059 group received PD98059 administration as well as EA treatment. We first sterilized the skin over the lumbar spine, and then injected PD98059 (Sigma-Aldrich, St. Louis, MO, USA), an inhibitor of extracellular regulated kinase (ERK), into the intervertebral space (lumbar 4–5) using a microsyringe, at a dose of 2.78 mg/kg.

Neurological function assessment

24 hours after reperfusion, a neurological assessment of the rats in the five different groups was performed by a blinded investigator using the 18-point scoring system reported by Garcia et al. (1995). The system consisted of the following six
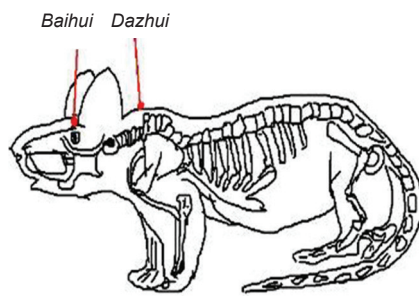
Figure 1 *Baihui* (DU20) and *Dazhui* (DU14) acupoints on the rat.

tests: (1) spontaneous activity, (2) symmetry in the movement of four limbs, (3) forepaw outstretching, (4) climbing, (5) body proprioception, and (6) response to vibrissae touch. The score given to each rat at the completion of the evaluation was the summation of all six individual test scores, with a minimum neurologic score of 3 and a maximum score of 18.

Measurement of infarct volume
After neurological evaluation, rats were decapitated, and the brains were rapidly removed and frozen to preserve morphology during slicing. Infarct volumes were measured as described previously (Walcott et al., 2012). In brief, the brain was rapidly dissected and sectioned into five coronal blocks of an approximate thickness of 2 mm, and stained with 2% (w/v) 2,3,5-triphenyltetrazolium chloride (TTC) (Sigma-Aldrich) for 30 minutes at 37°C, followed by overnight immersion in 4% (w/v) paraformaldehyde. The infarct area in each slice was demarcated and analyzed using Image J software (National Institutes of Health, Bethesda, MD, USA). The infarct volumes were calculated with the following formula: (total contralateral hemispheric volume−total ipsilateral hemispheric stained volume) / (total contralateral hemispheric volume) × 100%.

Histopathological examination
Hematoxylin-eosin (HE) staining was performed to show the morphological features of injured neurons in the cerebral cortex. 24 hours after MCAO, rats were sacrificed, and the brains were fixed by transcardial perfusion with saline solution, followed by perfusion and immersion in 4% paraformaldehyde. Brains were then dehydrated in a graded series of alcohols and embedded in paraffin. A series of 5-μm-thick sections were cut from the block. Finally, the sections were stained with HE reagents. The slices were observed and photographed with an Olympus BX50 microscope (Tokyo, Japan).

Transmission electron microscopy
Transmission electron microscopy was performed at 24 hours after MCAO. The cortex was cut into 1-mm³ cubes and fixed in 1% paraformaldehyde/2.5% glutaraldehyde for 24 hours. Samples were then fixed for 2 hours in 1% osmium tetroxide and dehydrated in a graded ethanol series and embedded in Araldite. The samples were cut into 50-nm-thick

Table 1 The primers used for quantitative real-time PCR

Gene	Primer sequence
Bcl-2	
Forward primer	5′-TGC GCT CAG CCC TGT G-3′
Reverse primer	5′-GGT AGC GAC GAG AGA AGT CAT C-3′
Probe	5′-CCA CCT GTG GTC CAC CTG-3′
Bax	
Forward primer	5′-CAA GAA GCT GAG CGA GTG TCT-3'
Reverse primer	5′-CAA TCA TCC TCT GCA GCT CCA T AT T-3'
Probe	5′-CCA GTT CAT CTC CAA TTC G-3'
GCSh	
Forward primer	5′-TAT CTG CCC AAT TGT TAT GGC TTT-3′
Reverse primer	5′-TCC TCC CGT GTT CTA TCA TCT ACA-3′
Probe	5′-CAT CGC CAT TTT ACC GAG GCT ACG TG-3′
GCSl	
Forward primer	5′-GGG CAC AGG TAA AAC CCA ATA G-3′
Reverse primer	5′-TTG GGT CAT TGT GAG TCA GTA GCT-3′
Probe	5′-TTAA TCT TGC CTC CTG CTG TGT GAT GCC-3′
Nrf2	
Forward primer	5′-CCA TTC CCG AGT TAC AGT GTC TT-3′
Reverse primer	5′-GAT CGA TGA GTA AAA ATG GTA ATT GC-3′
Probe	5′-CAG CCC AGA GGC CAC ACT GAC AGA-3′
GAPDH	
Forward primer	5′-CCT CAA GAT TGT CAG CAA TGC A-3′
Reverse primer	5′-TGG CAG TGA TGG CAT GGA-3′
Probe	5′-CAC CAC CAA CTG CTT AGC CCC CCT-3′

sections and stained with uranylacetate and lead citrate. The ultrastructure of pyramidal cells, astrocytes and blood-brain barrier (BBB) were observed with a Tecnai 12 transmission electron microscope (Philips, Eindhoven, Netherlands).

Quantitative real-time PCR
24 hours after MCAO, rats were sacrificed, and the ischemic cortex of the ipsilateral hemisphere was dissected. Total RNA was extracted using TRIzol reagent (Invitrogen, Carlsbad, CA, USA) according to the manufacturer's protocol. cDNA synthesis was performed using random hexamer primers and the TaqMan reverse transcription kit (Applied Biosystems, Foster City, CA, USA). Samples were subjected to real-time PCR analysis on a 7500 Sequence Detection System (Applied Biosystems) in accordance with the manufacturer's instructions. The primers and probes for rat *Bax*, *Bcl-2*, *GCSh*, GCSl, *Nrf2* and *GAPDH* were designed with Primer Express 3.0 software (Applied Biosystems) using GenBank accession numbers. The primers are listed in **Table 1**. GAPDH was used as an internal control. mRNA quantities were calculated according to standard curves. Each sample was assayed in triplicate.

Measurement of glutathione reductase, glutathione and glutathione peroxidase
The blood samples were centrifuged at 3,000 × *g*, 4°C, for 15 minutes, and serum was extracted and stored at −80°C until analysis. The glutathione reductase (GR), glutathione (GSH) and glutathione peroxidase (GSH-Px) activities in the serum
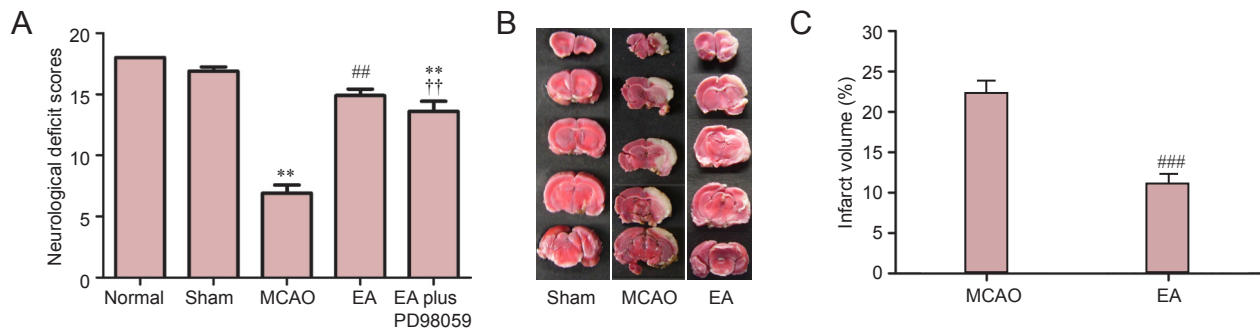
Figure 2 EA attenuates neurological deficits in rats with MCAO.
(A) Neurological function scores 24 hours after reperfusion (n = 10 per group). A higher score indicates better neurological function. Representative 2,3,5-triphenyltetrazolium chloride (TTC) staining (B) and volume (%) (C) of the cerebral infarct in the rat brain (n = 5 per group). The infarcted tissue remained unstained (white), whereas normal tissue stained red. Results are expressed as the mean ± SEM. Paired *t*-test was used for comparing cerebral infarct volume, while one-way analysis of variance (ANOVA) followed by Tukey's multiple comparisons test was used for comparing neurological deficit scores. **$P < 0.01$, *vs.* sham (sham-operation) group; ##$P < 0.01$, ###$P < 0.001$, *vs.* MCAO group; ††$P < 0.01$, *vs.* EA (MCAO + EA) group. MCAO: Middle cerebral artery occlusion; EA: electroacupuncture; EA plus PD98059: MCAO + EA + PD98059.
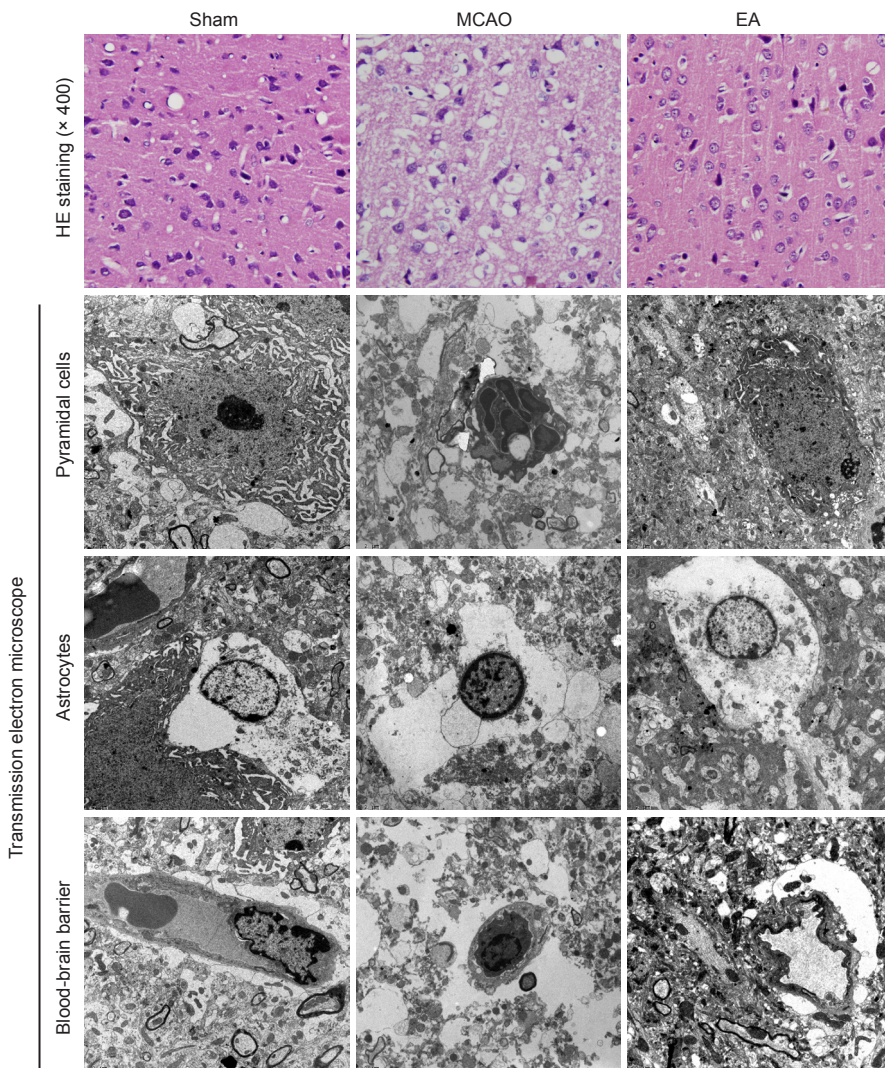

Figure 3 Evaluation of histopathological changes.

HE staining was performed on sections from the ischemic cortex 24 hours after reperfusion in the sham (sham-operation), MCAO and EA (MCAO + EA) groups (n = 5 per group). There were no obvious pathological changes in rats in the sham group. In comparison, pyramidal cells in the MCAO group were disordered and sparsely distributed. In the EA group, edema was alleviated, and the loss of neurons and structural abnormalities were reduced in the cortex. Ultrastructural changes were observed by transmission electron microscope (× 5,800). Images show the ultrastructural changes in pyramidal cells, astrocytes and the blood-brain barrier (BBB) 24 hours after reperfusion in the different groups (n = 3 per group). The pyramidal cells in the sham group were characterized by a round nucleus, and a clear nucleolus and cytoplasm. In contrast, pyramidal cells in the MCAO group displayed a shrunken nucleus, swollen or ganelles and chromatin condensation. In the EA group, edema was reduced, and the organelles, cytoplasm and vasculature showed fewer pathological changes. MCAO: Middle cerebral artery occlusion; EA: electroacupuncture; HE: hematoxylin-eosin.

were measured using commercial kits (Jiancheng Bioengineering Institute, Nanjing, Jiangsu, China). The levels of GR, GSH and GSH-Px were expressed as units (U) /mg protein, mg/L and U, respectively.

Immunohistochemistry

Immunohistochemical analysis was performed to evaluate GCS and Nrf2 expression in brain cells 24 hours after MCAO. Cerebral cortical tissue samples were fixed in 4%

paraformaldehyde overnight at room temperature. A series of 4–6-mm-thick tissue blocks were cut into five sections. The sections were deparaffinized and treated with 3% H_2O_2/methanol solution, followed by blocking with 5% goat serum in Tris-buffered saline. Then, the sections were incubated with rabbit anti-rat GCS monoclonal antibody (1:100; BA1627, Wuhan Boster Biotechnology Company, Wuhan, Hubei Province, China) or rabbit anti-rat *Nrf2* monoclonal antibody(1:150; PB0327, Wuhan Boster Biotechnology Company), as the primary antibody, and then with horseradish peroxidase-conjugated goat anti-rabbit IgG, as the secondary antibody (1:100; BA1055, Wuhan Boster Biotechnology Company). After the sections were stained with DAB, images were acquired on a light microscope (Leica DM4000, Wetzlar, Germany) at 400× magnification. Morphometric analysis was performed in a blinded manner by two independent investigators. For each section, five visual fields were chosen at random for statistical analysis. Results were expressed as the mean optical density of the GCS or Nrf2 positive cells.

Statistical analysis
Data are expressed as the mean ± SEM and were analyzed with SPSS 13.0 for Windows (SPSS, Chicago, IL, USA). Paired *t*-test was used to compare cerebral infarct volumes, while one-way analysis of variance (ANOVA) followed by Tukey's multiple comparisons test was used for multiple comparisons. $P < 0.05$ was considered statistically significant.

Results
EA alleviated neurological deficits after I/R in rats
To investigate whether EA improves neurological function in the rat model of MCAO, neurological testing was performed. After 2 hours of ischemia followed by 24 hours of reperfusion, rats subjected to MCAO exhibited significant motor deficits. Neurological function scores were significantly decreased in the MCAO group ($P < 0.01$; **Figure 2A**). Rats receiving EA showed significant improvements in neurological function compared with the MCAO group ($P < 0.01$; **Figure 2A**). To assess whether the ERK1/2 signaling pathway participates in the neuroprotective effect of EA, PD98059 (a specific ERK1/2 inhibitor) was used to block ERK1/2 signaling. As shown in **Figure 2A**, we found that the improvement in neurological function produced by EA was significantly abrogated in the EA plus PD98059 group, compared with the EA group ($P < 0.01$). This result suggests that EA attenuates neurological deficits *via* the ERK1/2 signaling pathway.

EA reduced infarct volume in the ischemic brain
Infarct volume, a measure of stroke severity (Liu et al., 2009), was also assessed in the different groups. Extensive infarction was detected by TTC staining in the cerebral cortex in rats subjected to MCAO (**Figure 2B**). Rats treated with EA had lower infarct volumes than animals in the MCAO group ($P < 0.001$, **Figure 2C**), confirming the neuroprotective effect of EA against cerebral I/R injury.

EA attenuated cerebral damage after cerebral I/R injury
The neuroprotective effect of EA against cerebral I/R damage was supported by HE staining and transmission electron microscopy. HE staining showed no obvious pathological changes in rats in the sham group—pyramidal cells were tightly arranged, cellular morphology was normal, parenchymal integrity was normal, with light staining, and the nucleoli were clear in the cortex. In contrast, in the MCAO group, cortical pyramidal cells were sparse and showed a disordered arrangement. Furthermore, there was neuronal loss, and edema was present with karyopyknosis, with deep staining, and the nucleoli were not clearly visible. In the EA group, compared with the MCAO group, although pyramidal cells displayed a disordered arrangement, their number was normal, and edema was reduced in the cortex. In addition, there were many neurons with a normal morphology, and some cells also had a clearly visible nucleolus (**Figure 3A**).

The ultrastructural changes in neurons and the BBB in the cerebral cortex observed by transmission electron microscopy are shown in **Figure 3B–D**. In the sham group, the pyramidal cells were characterized by around nucleus, evenly distributed chromatin, and a clear nucleolus and cytoplasm. The vascular endothelial cells had smooth and flat surfaces, and the endothelia, basement membranes and foot processes were in close contact. In contrast, pyramidal cells in the MCAO group displayed a shrunken nucleus, swollen organelles, chromatin condensation and marginalization, and the formation of apoptotic bodies. Vacuoles around small vessels were also observed. The glial cells around these vacuoles were not clearly detectable, and the inner surfaces of the blood vessels appeared rough. At high power, the endothelial cells appeared swollen, and the thickened basement membrane was not well organized. In the EA group, edema was reduced, and the organelles, cytoplasm and vasculature showed fewer pathological changes. Furthermore, the nuclei in neurons and glial cells appeared more normal. The vascular endothelial cells and the basement membrane exhibited smooth and intact surfaces with clear layers.

EA inhibited apoptosis following cerebral I/R
The proto-oncoproteins Bcl-2 and Bax are key regulators of the mitochondrial apoptotic pathway that is initiated by a variety of extracellular and intracellular stressors (Ferrer and Planas, 2003). To explore whether EA has anti-apoptotic effects, the mRNA expression of Bax and Bcl-2 in the ischemic cerebral cortex were investigated by real-time PCR after 24 hours of reperfusion. The MCAO group had significantly higher mRNA expression of Bax than the sham group ($P < 0.05$). Compared with the MCAO group, EA treatment significantly reduced Bax mRNA expression and increased *Bcl-2* mRNA expression, and it increased the Bcl-2/Bax ratio in the ischemic cortex ($P < 0.05$; **Figure 4**).

EA upregulated endogenous antioxidant systems following I/R
To further explore the mechanisms underlying the neuroprotective effect of EA, the levels of GR, GSH and GSH-Px

in serum were measured to examine the oxidative response 24 hours after ischemia. GR, GSH and GSH-Px levels were significantly lower in the MCAO group compared with the sham group ($P < 0.05$). However, GSH, GSH-Px and GR levels were significantly higher in the EA group, compared with the MCAO group ($P < 0.05$). In addition, a substantial reduction in GR and GSH-Px activities was observed in the EA plus PD98059 group, compared with the EA group ($P < 0.05$, **Figure 5**).

EA enhanced the expression levels of GCS and Nrf2 in the cortex of rats with cerebral ischemia and reperfusion injury
Nuclear factor-E2-related factor 2 (Nrf2) is a key transcription factor that regulates antioxidant genes in the adaptive response to oxidative stress (Ma et al., 2015). To identify whether Nrf2/GCS signaling is involved in the neuroprotective effect of EA, the ischemic cortex was analyzed by real-time PCR and immunohistochemistry. Real-time PCR analysis 24 hours following reperfusion showed that mRNA levels of *GCSh* and *GCSl* were significantly higher in rats in the EA group compared with rats in the MCAO group ($P < 0.05$). However, there was no significant difference in *Nrf2* expression between the EA and MCAO groups. Moreover, in rats in the EA plus PD98059 group, there was a remarkable decrease in *GCSh* mRNA levels compared with the EA group ($P < 0.05$, **Figure 4D–F**).

Changes in expression of Nrf2 and GCS in the cortex were also analyzed by immunohistochemistry. The mean optical densities of Nrf2 and GCS-positive cells were higher in the EA group compared with the MCAO group ($P < 0.01$). The mean optical densities of Nrf2 and GCS-positive cells were lower in the EA plus PD98059 group compared with the EA group ($P < 0.01$, **Figure 6**).

Discussion
In the current study, we found that EA protects the brain against I/R injury in rats subjected to MCAO. Notably, we found that the neuroprotective effect of EA is associated with the maintenance of the antioxidant system. Moreover, specific inhibition of the ERK1/2 pathway abolished the EA-induced increase in Nrf2 and GCS expression. Taken together, these findings suggest that EA attenuates cerebral I/R injury by activating the ERK1/2 signaling pathway and inducing Nrf2/GCS expression.

Apoptosis is thought to be pivotal in neuronal injury following cerebral I/R (Chen et al., 2014; Ji et al., 2014). Neuronal death or survival depends on the balance between pro-apoptotic (Bax) and anti-apoptotic (Bcl-2 and Bcl-xL) proteins during cerebral ischemia (Zhu et al., 1999; Sun et al., 2010). It is well known that the increase in brain damage is associated with increased apoptosis, as indicated by increased levels of Bax and decreased levels of Bcl-2. Accumulating evidence shows that the inhibition of apoptosis has a beneficial effect in acute ischemic stroke. For example, antisense knockdown of endogenous Bcl-2 exacerbates cerebral ischemic injury in rats and blocks the neuroprotection afforded by ischemic preconditioning (Chen et al., 2000; Shimizu et

al., 2001). We observed a great number of apoptotic neurons in the brain of rats with MCAO 24 hours after reperfusion, and there was also a significant upregulation of *Bax* and a downregulation of *Bcl-2*. This is consistent with previous reports (Chen et al., 2015; Jie et al., 2015). Furthermore, we found that EA upregulated the anti-apoptotic protein *Bcl-2* and downregulated the pro-apoptotic protein *Bax*, and reduced neuronal apoptosis. Further studies are required to clarify the mechanisms underlying the regulation of apoptosis by EA.

An imbalance between oxidative stress and antioxidant defense systems appears to play an important role in ischemic stroke injury (Love, 1999). GSH-Px, GR and superoxide dismutase (SOD) are the first line of defense against cerebral ischemic injury (Kontos, 2001). To clarify the effects of EA on oxidative stress induced by I/R injury, we measured the levels of GR, GSH-Px and GSH. EA restored GR, GSH and GSH-Px, suggesting that EA has an important anti-oxidative effect in I/R.

Nrf2, a key regulator of cell survival, has been implicated in the regulation of several key antioxidant enzymes such as γ-GCS, which plays an important role in antioxidant defense (Ma et al., 2015). We found that EA increases GSH content, and upregulated the expression of γ-GCS, the rate-limiting enzyme in GSH biosynthesis. Given that these genes are regulated by Nrf2, we infer that Nrf2 is a potential mediator of the neuroprotective effects of EA. Recent findings show that activation of Nrf2 significantly reduces the damage produced by ischemic stroke, suggesting that Nrf2 may represent a potential target for neuroprotection after cerebral ischemia (Zhao et al., 2011). In this study, EA significantly increased the expression of Nrf2 and GCS in the ischemic cortex 24 hours after MCAO, suggesting that the neuroprotective effect of EA might be associated with the upregulation of Nrf2 and GCS.

MAPK, including p38 MAPK, ERK1/2 and c-Jun N-terminal kinase (JNK) are considered to have critical roles in cerebral ischemia (Zhu et al., 2014). Studies have shown that p38 MAPK in the cortex and hippocampus exerted neuroprotective effects against ischemic brain injury (Zheng and Zuo, 2004; Blanquet et al., 2009; Zhao et al., 2013). Several reports have shown that p38 MAPK upregulated the expression of Bcl-2 and Bcl-xL in cerebral ischemic preconditioning models (Guan et al., 2014; Cheng et al., 2015). In addition, the PI3K/Akt and MAPK pathways activate the Nrf2 pathway (Jung and Kwak, 2010; Gong et al., 2015). Furthermore, the PI3K inhibitor LY294002 abolishes Nrf2 activation and heme oxygenase 1 (HO-1) induction (Qi et al., 2012). Previous studies have demonstrated that EA stimulation exerted neuroprotective effects against cerebral I/R injury by activating the ERK1/2 signaling pathway (Du et al., 2010; Xie et al., 2013; Huang et al., 2014). Taken together, these findings indicate that the ERK1/2 signaling pathway may be involved in the anti-apoptotic process and the activation of Nrf2. However, the mechanisms by which EA activates the Nrf2 pathway are unclear and require further investigation.
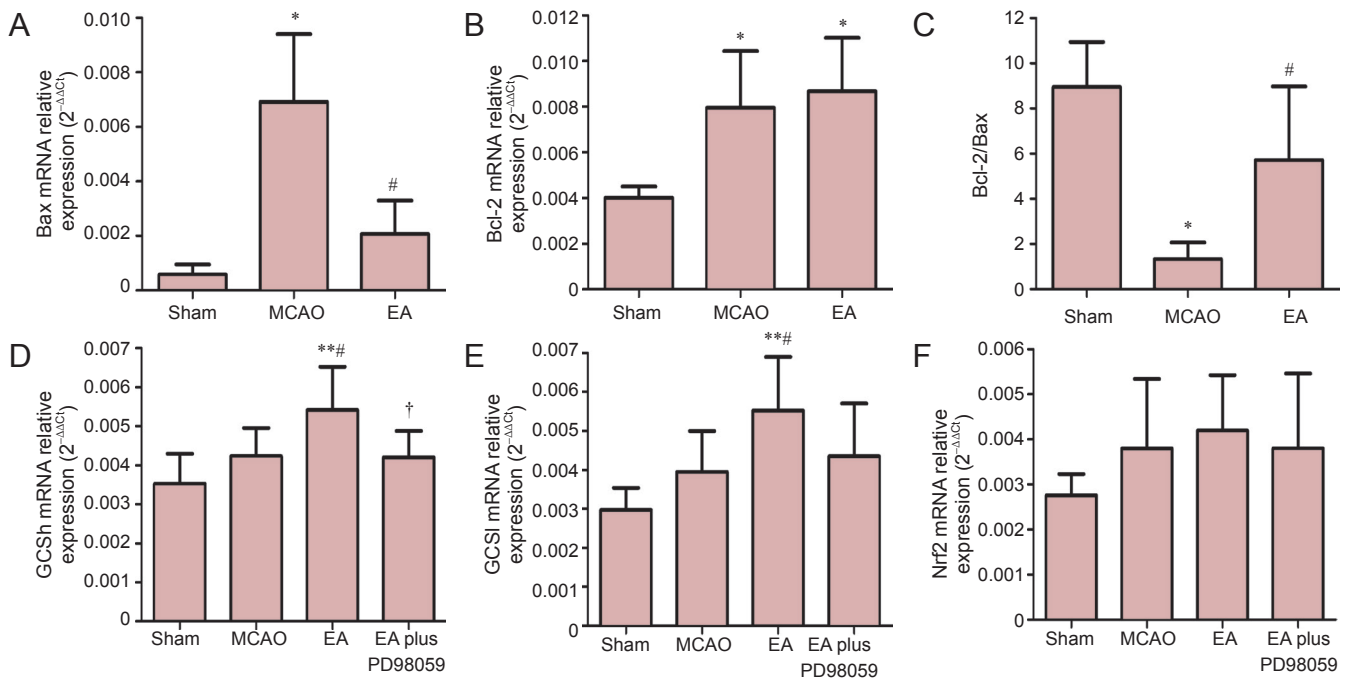
Figure 4 Effects of EA on mRNA expression levels of Bax, Bcl-2, GCS and Nrf2 in the ischemic cortex after MCAO.
Bax (A), Bcl-2 (B), GCSh (D), GCSl (E) and Nrf2 (F) mRNA expression levels, as assessed by real-time PCR. The *Bax/Bcl-2* ratio is shown in C. Data ($n = 7$ per group in A–C, $n = 5$ per group in D–F) are expressed as the mean ± SEM. Statistical significance was determined using analysis of variance followed by Tukey's multiple comparison test for multiple comparisons. *$P < 0.05$, **$P < 0.01$, *vs.* sham (sham-operation) group; #$P < 0.05$, *vs.* MCAO group; †$P < 0.05$, *vs.* EA (MCAO + EA) group. MCAO: Middle cerebral artery occlusion; EA: electroacupuncture; EA plus PD98059: MCAO + EA + PD98059; GCSh: gamma-glutamylcysteine synthetase heavy subunit; GCSl: gamma-glutamylcysteine synthetase light subunit; Nrf2: nuclear factor erythroid 2-related factor 2.
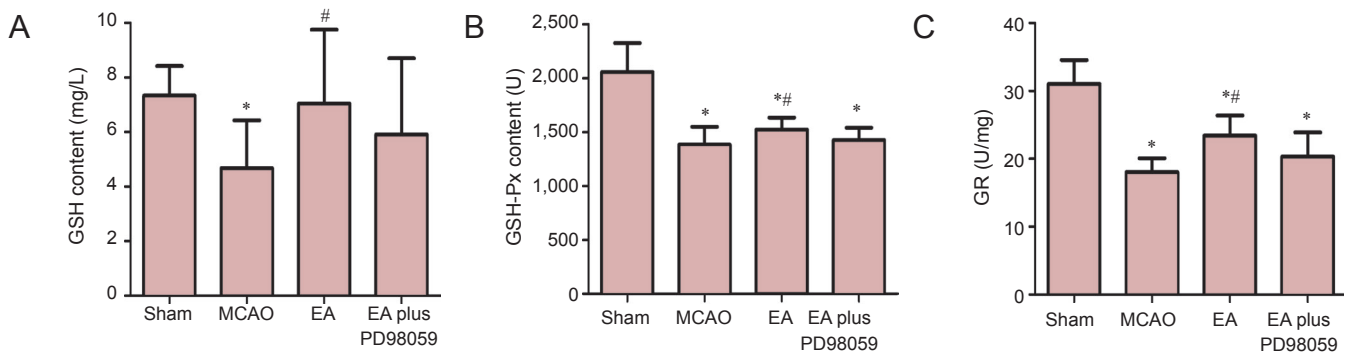

Figure 5 Effects of EA on serum GR, GSH and GSH-Px levels.
EA significantly increased the GSH (A), GSH-Px (B) and GR (C) levels, compared with the MCAO group ($n = 10$ animals per group). Data are expressed as the mean ± SEM. Statistical significance was determined using analysis of variance followed by Tukey's multiple comparison test for multiple comparisons. *$P < 0.05$, *vs.* sham (sham-operation) group; #$P < 0.05$, *vs.* MCAO group. MCAO: Middle cerebral artery occlusion; EA: electroacupuncture; GR: glutathione reductase; GSH: glutathione; GSH-Px: glutathione peroxidase; EA plus PD98059: MCAO + EA + PD98059.

Studies have shown that EA stimulation, of different acu-points and at various frequencies, exerts neuroprotective effects against cerebral I/R injury in rats with MCAO. For example, EA stimulation at the *Baihui* acupoint (2/15 Hz) exerts anti-apoptotic and neuroprotective effects by increasing Bcl-2 expression and reducing glutamate toxicity (Zhu et al., 2013). EA stimulation (3 Hz) also improves behavioral performance by enhancing brain-derived neurotrophic factor production (Kim et al., 2012). Tian et al. (2015) demonstrated that EA stimulation at the *Baihui*, *Mingmen* (DU4) and *Zusanli* (ST36) acupoints (30/50 Hz) provided neuroprotection against brain edema in rats with MCAO. In this study, we chose the *Baihui* and *Dazhui* acupoints, based on our clinical experience (Li, 2007). EA stimulation at the *Baihui* acupoint improves nerve and periosteum function, enhances dredging, activates the *Du* meridian, and revives the brain. Moreover, EA stimulation at the *Dazhui* acupoint improves blood circulation to dissipate blood stasis, enhances brain function and alleviates brain disease. Our findings suggest that EA stimulation at *Baihui* and *Dazhui* acupoints, at a frequency of 3Hz, also exerts neuroprotective effects against cerebral I/R injury.

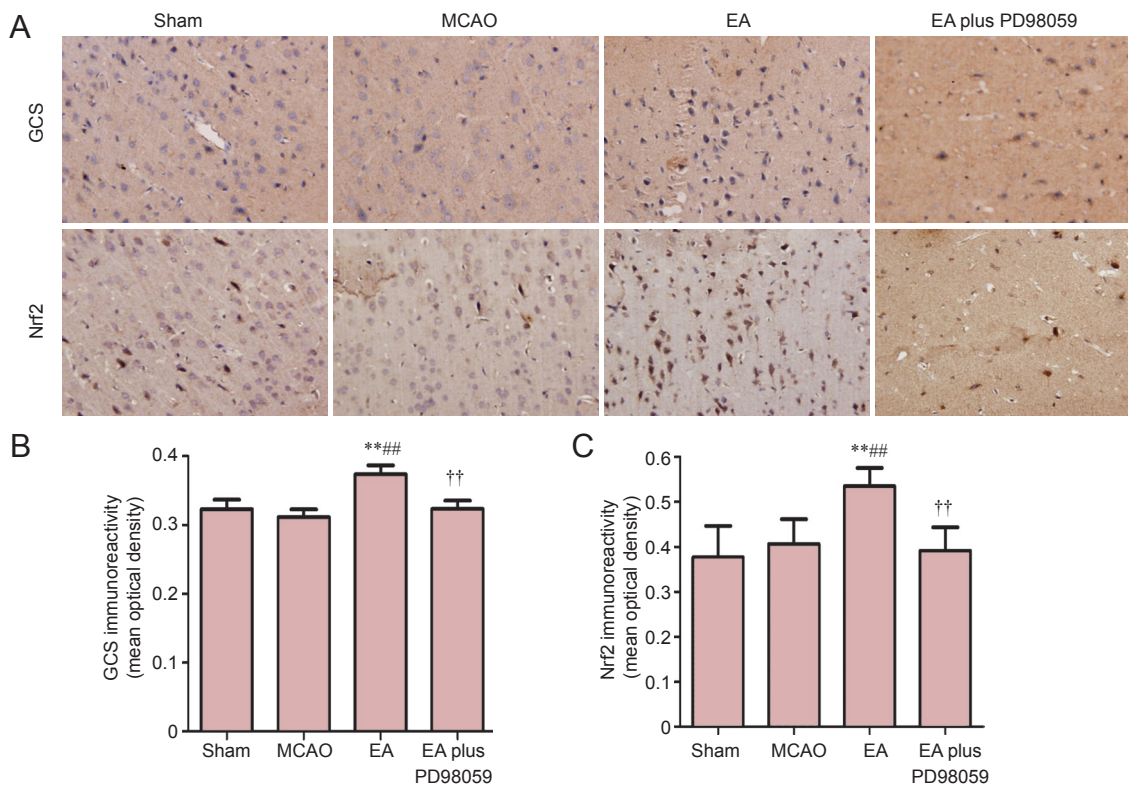Our findings demonstrate that EA provides neuroprotection against cerebral I/R *via* activation of the ERK1/2

Figure 6 Effects of EA on GCS and Nrf2 immunoreactivities in the ischemic cortex.
(A) Immunohistochemical staining for GCS and Nrf2 in the cortex in the different groups ($\times$ 400) (n = 5 per group). (B, C) Mean optical densities of GCS and Nrf2-immunoreactive cells. Data are expressed as the mean $\pm$ SEM. Paired *t*-test was used to compare two groups, while analysis of variance followed by Tukey's multiple comparisons test was used for multiple comparisons. **$P < 0.01$, *vs.* sham (sham-operation) group; ##$P < 0.01$, *vs.* MCAO group; ††$P < 0.01$, *vs.* EA (MCAO + EA) group. EA: Electroacupuncture; GCS: glutamylcysteine synthetase; Nrf2: nuclear factor erythroid 2-related factor 2; MCAO: middle cerebral artery occlusion; EA plus PD98059: MCAO + EA + PD98059.

pathway. The potent efficacy of EA in protecting against focal cerebral I/R injury makes EA a promising therapeutic strategy for stroke. However, the role of ERK1/2/Nrf2 in the neuroprotective effects of EA and the mechanisms by which EA affects the expression of Nrf2 are unclear and require further study. Moreover, additional research is needed to elucidate whether other signaling pathways and factors contribute to the neuroprotective effects of EA. Nonetheless, our study suggests that the ERK1/2 pathway plays a major role in neuroprotection against cerebral I/R injury.

References

Allen CL, Bayraktutan U (2009) Oxidative stress and its role in the pathogenesis of ischaemic stroke. Int J Stroke 4:461-470.

Blanquet PR, Mariani J, Fournier B (2009) Temporal assessment of histone H3 phospho-acetylation and casein kinase 2 activation in dentate gyrus from ischemic rats. Brain Res 1302:10-20.

Chen J, Simon RP, Nagayama T, Zhu R, Loeffert JE, Watkins SC, Graham SH (2000) Suppression of endogenous bcl-2 expression by anti-sense treatment exacerbates ischemic neuronal death. J Cereb Blood Flow Metab 20:1033-1039.

Chen W, Xu B, Xiao A, Liu L, Fang X, Liu R, Turlova E, Barszczyk A, Zhong X, Sun CL, Britto LR, Feng ZP, Sun HS (2015) TRPM7 inhibitor carvacrol protects brain from neonatal hypoxic-ischemic injury. Mol Brain 8:11.

Chen WQ, Sun YY, Liu KY, Sun XJ (2014) Autophagy: a double-edged sword for neuronal survival after cerebral ischemia. Neural Regen Res 9:1210-1216.

Cheng CY, Lin JG, Tang NY, Kao ST, Hsieh CL (2015) Electroacupuncture at different frequencies (5 Hz and 25 Hz) ameliorates cerebral ischemia-reperfusion injury in rats: possible involvement of p38 MAPK-mediated anti-apoptotic signaling pathways. BMC Complement Altern Med 15:241.

Deb P, Sharma S, Hassan KM (2010) Pathophysiologic mechanisms of acute ischemic stroke: An overview with emphasis on therapeutic significance beyond thrombolysis. Pathophysiology 17:197-218.

Donnan GA, Fisher M, Macleod M, Davis SM (2008) Stroke. Lancet 371:1612-1623.

Du J, Wang Q, Hu B, Peng Z, Zhao Y, Ma L, Xiong L, Lu Y, Zhu X, Chen S (2010) Involvement of ERK 1/2 activation in electroacupuncture pretreatment via cannabinoid CB1 receptor in rats. Brain Res 1360:1-7.

Ferrer I, Planas AM (2003) Signaling of cell death and cell survival following focal cerebral ischemia: life and death struggle in the penumbra. J Neuropathol Exp Neurol 62:329-339.

Garcia JH, Wagner S, Liu KF, Hu XJ (1995) Neurological deficit and extent of neuronal necrosis attributable to middle cerebral artery occlusion in rats. Statistical validation. Stroke 26:627-635.

Gong X, Ivanov VN, Hei TK (2015) 2,3,5,6-Tetramethylpyrazine (TMP) down-regulated arsenic-induced heme oxygenase-1 and ARS2 expression by inhibiting Nrf2, NF-κB, AP-1 and MAPK pathways in human proximal tubular cells. Arch Toxicol doi: 10.1007/s00204-015-1600-z.

Guan J, Li H, Lv T, Chen D, Yuan Y, Qu S (2014) Bone morphogenic protein-7 contributes to cerebral ischemic preconditioning induced-ischemic tolerance by activating p38 mitogen-activated protein kinase signaling pathway. Inflammation 37:1289-1296.

Huang J, Ye X, You Y, Liu W, Gao Y, Yang S, Peng J, Hong Z, Tao J, Chen L (2014) Electroacupuncture promotes neural cell proliferation in vivo through activation of the ERK1/2 signaling pathway. Int J Mol Med 33:1547-1553.

Ji XY, Zhang LN, Liu R, Liu YZ, Song JF, Dong H, Jia YF, Zhou ZG (2014) Potential targets for protecting against hippocampal cell apoptosis after transient cerebral ischemia-reperfusion injury in aged rats. Neural Regen Res 9:1122-1128.

Jie P, Hong Z, Tian Y, Li Y, Lin L, Zhou L, Du Y, Chen L, Chen L (2015) Activation of transient receptor potential vanilloid 4 induces apoptosis in hippocampus through downregulating PI3K/Akt and upregulating p38 MAPK signaling pathways. Cell Death Dis 6:e1775.

Jung KA, Kwak MK (2010) The Nrf2 system as a potential target for the development of indirect antioxidants. Molecules 15:7266-7291.

Kim MW, Chung YC, Jung HC, Park MS, Han YM, Chung YA, Maeng LS, Park SI, Lim J, Im WS, Chung JY, Kim M, Mook I, Kim M (2012) Electroacupuncture enhances motor recovery performance with brain-derived neurotrophic factor expression in rats with cerebral infarction. Acupunct Med 30:222-226.

Kontos HA (2001) Oxygen radicals in cerebral ischemia: the 2001 Willis lecture. Stroke 32:2712-2716.

Kuluz JW, Prado RJ, Dietrich WD, Schleien CL, Watson BD (1993) The effect of nitric oxide synthase inhibition on infarct volume after reversible focal cerebral ischemia in conscious rats. Stroke 24:2023-2029.

Li P, Tjen-A-Looi SC, Guo ZL, Longhurst JC (2010) An arcuate-ventrolateral periaqueductal gray reciprocal circuit participates in electroacupuncture cardiovascular inhibition. Auton Neurosci 158:13-23.

Li Z (2007) Experimental Acupuncturology. Beijing: China Press of Traditional Chinese Medicine.

Li ZR, Cui L (2006) Application of TC index location on Longa's animal model of regional experimental cerebral ischemia and reperfusion. Zhongguo Zhong Xi Yi Jie He Za Zhi 26 Suppl:18-20.

Li ZR, Shen MH, Peng YJ (2005) Progress in researches on the effect of acupuncture in antagonizing oxygen stress. Chin J Integr Med 11:156-160.

Liu F, Schafer DP, McCullough LD (2009) TTC, Fluoro-Jade B and NeuN staining confirm evolving phases of infarction induced by Middle Cerebral Artery Occlusion. J Neurosci Methods 179:1-8.

Love S (1999) Oxidative stress in brain ischemia. Brain Pathol 9:119-131.

Lv E, Deng J, Yu Y, Wang Y, Gong X, Jia J, Wang X (2015) Nrf2-ARE signals mediated the anti-oxidative action of electroacupuncture in an MPTP mouse model of Parkinson's disease. Free Radic Res 49:1296-1307.

Ma WW, Li CQ, Yu HL, Zhang DD, Xi YD, Han J, Liu QR, Xiao R (2015) The oxysterol 27-hydroxycholesterol increases oxidative stress and regulate Nrf2 signaling pathway in astrocyte cells. Neurochem Res 40:758-766.

Qi H, Han Y, Rong J (2012) Potential roles of PI3K/Akt and Nrf2–Keap1 pathways in regulating hormesis of Z-ligustilide in PC12 cells against oxygen and glucose deprivation. Neuropharmacology 62:1659-1670.

Renfu Q, Rongliang C, Mengxuan D, Liang Z, Jinwei X, Zongbao Y, Disheng Y (2014) Anti-apoptotic signal transduction mechanism of electroacupuncture in acute spinal cord injury. Acupunct Med 32:463-471.

Russo T, Felzani G, Marini C (2011) Stroke in the very old: a systematic review of studies on incidence, outcome, and resource use. J Aging Res 2011:108785.

Shimizu S, Nagayama T, Jin KL, Zhu L, Loeffert JE, Watkins SC, Graham SH, Simon RP (2001) bcl-2 Antisense treatment prevents induction of tolerance to focal ischemia in the rat brain. J Cereb Blood Flow Metab 21:233-243.

Sun M, Gu Y, Zhao Y, Xu C (2010) Protective functions of taurine against experimental stroke through depressing mitochondria-mediated cell death in rats. Amino Acids 40:1419-1429.

Tian WQ, Peng YG, Cui SY, Yao FZ, Li BG (2015) Effects of electroacupuncture of different intensities on energy metabolism of mitochondria of brain cells in rats with cerebral ischemia-reperfusion injury. Chin J Integr Med 21:618-623.

Tjen-A-Looi SC, Li P, Longhurst JC (2006) Midbrain vlPAG inhibits rVLM cardiovascular sympathoexcitatory responses during electroacupuncture. Am J Physiol Heart Circ Physiol 290:H2543-2553.

Walcott BP, Kahle KT, Simard JM (2012) Novel treatment targets for cerebral edema. Neurotherapeutics 9:65-72.

Wang JY, Chen SP, Gao YH, Zhang JL, Liu JL (2015) Effect of repeated electroacupuncture intervention on hippocampal erk and p38mapk signaling in neuropathic pain rats. Evid Based Complement Alternat Med 2015:641286.

Wang Q, Li X, Chen Y, Wang F, Yang Q, Chen S, Min Y, Li X, Xiong L (2011) Activation of epsilon protein kinase C-mediated anti-apoptosis is involved in rapid tolerance induced by electroacupuncture pretreatment through cannabinoid receptor type 1. Stroke 42:389-396.

Wu P, Mills E, Moher D, Seely D (2010) Acupuncture in poststroke rehabilitation: a systematic review and meta-analysis of randomized tria. Stroke 41:e171-179.

Xie G, Yang S, Chen A, Lan LAN, Lin Z, Gao Y, Huang JIA, Lin J, Peng JUN, Tao J, Chen L (2013) Electroacupuncture at Quchi and Zusanli treats cerebral ischemia-reperfusion injury through activation of ERK signaling. Exp Ther Med 5:1593-1597.

Yu JB, Shi J, Gong LR, Dong SA, Xu Y, Zhang Y, Cao XS, Wu LL (2014) Role of Nrf2/ARE pathway in protective effect of electroacupuncture against endotoxic shock-induced acute lung injury in rabbits. PLoS One 9:e104924.

Yu JB, Shi J, Zhang Y, Gong LR, Dong SA, Cao XS, Wu LL, Wu LN (2015) Electroacupuncture ameliorates acute renal injury in lipopolysaccharide-stimulated rabbits via induction of HO-1 through the PI3K/Akt/Nrf2 pathways. PLoS One 10:e0141622.

Zhao L, Liu X, Liang J, Han S, Wang Y, Yin Y, Luo Y, Li J (2013) Phosphorylation of p38 MAPK mediates hypoxic preconditioning-induced neuroprotection against cerebral ischemic injury via mitochondria translocation of Bcl-xL in mice. Brain Res 1503:78-88.

Zhao Z, Chen Y, Wang J, Sternberg P, Freeman ML, Grossniklaus HE, Cai J (2011) Age-related retinopathy in NRF2-deficient mice. PLoS One 6:e19456.

Zheng S, Zuo Z (2004) Isoflurane preconditioning induces neuroprotection against ischemia via activation of P38 mitogen-activated protein kinases. Mol Pharmacol 65:1172-1180.

Zhou H, Zhang Z, Wei H, Wang F, Guo F, Gao Z, Marsicano G, Wang Q, Xiong L (2013) Activation of STAT3 is involved in neuroprotection by electroacupuncture pretreatment via cannabinoid CB1 receptors in rats. Brain Res 1529:154-164.

Zhu P, Zhan L, Zhu T, Liang D, Hu J, Sun W, Hou Q, Zhou H, Wu B, Wang Y, Xu E (2014) The roles of p38 MAPK/MSK1 signaling pathway in the neuroprotection of hypoxic postconditioning against transient global cerebral ischemia in adult rats. Mol Neurobiol 49:1338-1349.

Zhu X, Yin J, Li L, Ma L, Tan H, Deng J, Chen S, Zuo Z (2013) Electroacupuncture preconditioning-induced neuroprotection may be mediated by glutamate transporter type 2. Neurochem Int 63:302-308.

Zhu Y, Prehn JH, Culmsee C, Krieglstein J (1999) The beta2-adrenoceptor agonist clenbuterol modulates Bcl-2, Bcl-xl and Bax protein expression following transient forebrain ischemia. Neuroscience 90:1255-1263.